Chapter 11

Bioactive Polyaryletherketone Composites

Ryan K. Roeder Ph.D. and Timothy L. Conrad B.S.

11.1 Introduction

As discussed in detail in previous chapters of this book, the clinical and commercial success of polyaryletherketone (PAEK) implants in interbody spinal fusion was enabled by several advantageous properties. PAEK polymers are generally biocompatible, bioinert, and radiolucent; PAEK polymers also exhibit a high strength and similar compliance to bone [1–3]. However, a potential clinical disadvantage is that PAEK alone is not bioactive. In spinal fusion, for example, autograft or recombinant human bone morphogenetic protein (e.g., rhBMP-2) is required for osteointegration and, ultimately, the formation of a bony fusion [2]. Another potential disadvantage of PAEK polymers is a limited ability to tailor mechanical properties for a particular implant design or to match peri-implant tissue. Calcium phosphate reinforcement particles can be used to simultaneously address both disadvantages by providing (1) bioactivity and (2) tailored mechanical properties.

The addition of calcium phosphates—such as hydroxyapatite (HA), β-tricalcium phosphate (β-TCP), and bioglass—to polymers offers a robust system to engineer implant biomaterials with tailored biological, mechanical, and surgical function [4,5]. The historical design rationale has been to reinforce a tough, biocompatible polymer matrix with a stiff, bioactive filler. This concept was first conceived and investigated by Bonfield and coworkers in the 1980s with the development of HA-reinforced high-density polyethylene (HDPE), which found clinical use under the trade name HAPEX™ in non-load-bearing otologic and maxillofacial implants [6–9]. The superior mechanical properties of PAEK relative to polyethylene, combined with the clinical and commercial success of PAEK spinal implants in the 1990s, have led to growing interest in bioactive PAEK composites over the last decade (Table 11.1), which will be reviewed in this chapter.

Therefore, the objective of this chapter is to introduce a paradigm for the design of bioactive PAEK composites for biomedical devices (Figs 11.1 and 11.2) while reviewing the work to date within the framework of that paradigm (Table 11.1). The design of bioactive PAEK composites is considered within the framework of processing–structure–property relationships common to materials science and engineering [10]. The processing, structure, and properties of the materials used in a biomedical device have great influence on the device performance (Fig. 11.1). Of course, the device design is also of great importance, but the materials are often chosen "off the shelf" from known commodities without designing the materials for optimal device performance. The policies and practices of the US Food and Drug Administration (FDA) pose limitations to the introduction of new materials, but in this case, PAEK and most calcium phosphates are well known to the FDA. The "simple" combination of PAEK and calcium phosphates offers wide ranging

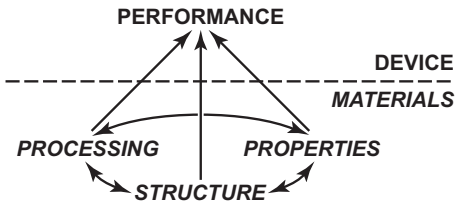

Figure 11.1 Schematic diagram illustrating the materials science and engineering paradigm of processing–structure–property relationships and their influence on the performance of biomedical devices.

PEEK Biomaterials Handbook. DOI: 10.1016/B978-1-4377-4463-7.10011-9

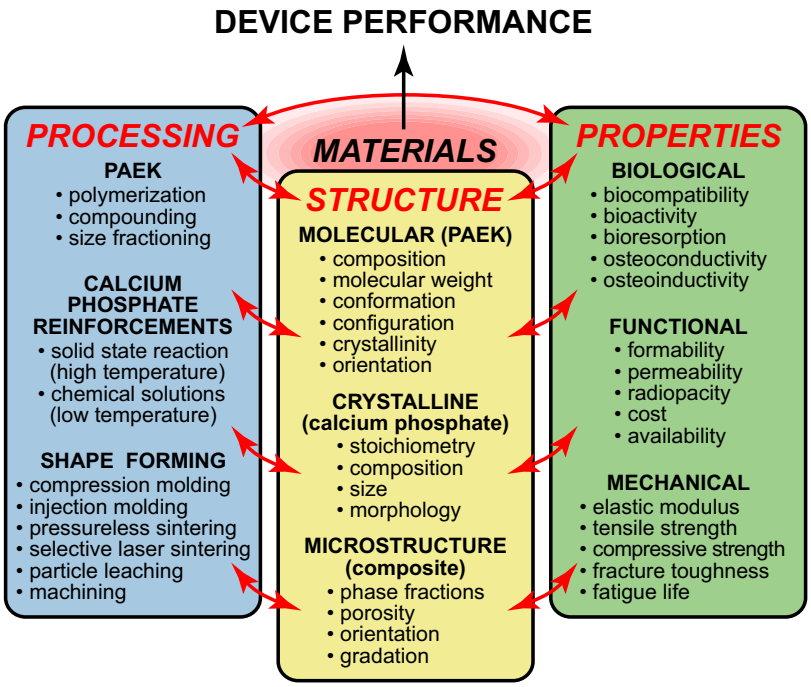

Figure 11.2 Schematic diagram showing a more detailed description of processing–structure–property relationships (Fig. 11.1) key to the design of calcium phosphate-reinforced PEEK composites for biomedical devices.

opportunities to design and manufacture bioactive composites with tailored properties (Fig. 11.2).

11.2 Processing–Structure Relationships

11.2.1 PAEK Synthesis and Structure

The processing of PAEK beads and powders of varying composition, molecular weight, size, and crystallinity has been reviewed in detail in preceding chapters of this book and elsewhere [3]. Investigations of bioactive PAEK composites to date have primarily utilized commercial polyetheretherketone (PEEK) beads and powders [11–26,30–35] manufactured by Victrex (150XF, 150PF, and 450G), and their subsidiary Invibio Biomaterial Solutions under the trade name PEEK-OPTIMA® (LT1PF and LT3UF) (Table 11.1). The 150 and LT3 grades have a number average molecular weight (M_n) of 83,000, while the 450 and LT1 grades have a number average molecular weight of 115,000. Powder grade PF, XF, and UF have a mass average particle diameter (D_{50}) of 50, 25, and 10 µm, respectively. A polyetherketoneketone (PEKK) powder with a mean particle size of 70 µm, manufactured by Oxford Performance Materials (OXPEKK-C), has also been investigated [27–30]. PEEK products are also currently available from Evonik Industries (VESTAKEEP®) and Solvay Advanced Polymers (KetaSpire® and Zeniva®) but have not yet been used in published reports for bioactive composites. The crystallinity of all the above products is generally in the range of 30–35% as-received. The crystallinity after molding will be discussed further in Section 11.2.3.

11.2.2 Bioactive Reinforcement Synthesis and Structure

Bioactive reinforcements or fillers have primarily utilized crystalline calcium orthophosphates, including stoichiometric HA [11–20,34], calcium-deficient HA [25–31], and β-TCP [21–24] (Table 11.1). However, strontium-substituted HA [32], amorphous calcium silicate [33], and Bioglass 45S5 [23,35] have also been investigated. These and a wide variety of other calcium phosphates are available for use as bioactive reinforcements (Table 11.2). A key aspect of selection is the solubility of a particular composition or stoichiometry, which influences biological properties and will be discussed further in Section 11.3.1.

High-temperature synthesis—including solid-state reactions, molten salt synthesis, and spray drying with calcination—generally leads to stoichiometric phases

Table 11.1 Summary of Investigations on Bioactive PEEK Composites

				Structure										
				PAEK			Calcium Phosphate				Porosity			
Years	Location	Refs.	Processing	Type	Supplier	Size, μm	Type	Morphology	vol%	Size, μm	vol%	Size, μm	Properties
1999–2004	Nanyang, Singapore[a]	[11–15]	Compounding + injection molding	PEEK	Victrex 450G	n/a	HA	Spray-dried spheres	0–40	~26 (3–100)	~0	n/a	Uniaxial tension (E, UTS, ε_f) uniaxial tension (N_f, σ_{fat}, E loss)
2003–2005	Nanyang, Singapore[a]	[16–18]	Selective laser sintering (SLS)	PEEK	Victrex 150XF	25	HA	Spray-dried spheres	0–22	<60 (90%)	70–74	n/r	Bioactivity in SBF, fibroblast adhesion
2005–2009	Nanyang, Singapore[a]	[19,20]	Cold press + sintering	PEEK	Victrex 150XF	25	HA	Spray-dried spheres	0–40	n/r	~0	n/a	UTS, UCS, bioactivity in SBF, OB adhesion
2006	Erlangen, Germany[b]	[21]	Compounding + injection molding	PEEK	Victrex 450G	n/a	β-TCP	~Equiaxed	0–22	<63 (98%)	~0	n/a	Uniaxial tension (E, UTS), OB proliferation
2006 –present	Erlangen, Germany[b]	[21–24]	SLS	PEEK	Victrex 150PF	50 (5–110)	β-TCP	~Equiaxed	4	<63 (98%)	n/r	n/r	OB culture; swine cranial defect histology and PS
2007 –present	Notre Dame, USA[c]	[25–27]	Compression molding	PEEK	Victrex 150XF	25	cdHA	Whiskers	0–50	~22 × 3	~0	n/a	Uniaxial tension (E, UTS, ε_f), ultrasound (C_{ij}), four-point bending (N_f, σ_{fat}, E loss)

(*Continued*)

Table 11.1 Summary of Investigations on Bioactive PEEK Composites—cont'd

				Structure										
				PAEK			Calcium Phosphate				Porosity			
Years	Location	Refs.	Processing	Type	Supplier	Size, μm	Type	Morphology	vol%	Size, μm	vol%	Size, μm	Properties
2009 −present	Notre Dame, USA[c]	[28–31]	Compression molding	PEKK	Oxford OXPEKK-C	70	cdHA	Whiskers	0–40	~22 × 3	75–90	200–500	Uniaxial compression (*E*, YS, ε_y), micro-CT, von Kossa
				PEEK	Invibio LT1PF, LT3UF	50, 10							
2009	Hong Kong[d]	[32]	Compression molding	PEEK	Victrex 150XF	25	HA, Sr–HA	~Equiaxed	0–30	~43 (45–75)	~0	n/a	Four-point bending (*E*, FS), bioactivity in SBF, OB proliferation, differentiation
2009	Nagoya, Japan[e]	[33]	Cold press + sintering	PEEK	Victrex 150XF	25	CaSi	~Equiaxed	0–50	~5	~0	n/a	Three-point bending (*E*, FS, ε_f), bioactivity in SBF

Structure: PEEK = polyetheretherketone; PEKK = polyetherketoneketone; HA = hydroxyapatite; β-TCP = β-tricalcium phosphate; cdHA = calcium-deficient HA; Sr-HA = strontium-doped HA; CaSi = calcium silicate, $CaO{\cdot}SiO_2$; n/a = not applicable; n/r = not reported.
Properties: E = *elastic modulus;* C_{ij} = *stiffness coefficients; UTS = ultimate tensile strength; UCS = ultimate compressive strength; YS = yield strength; FS = flexural strength; PS = push-out strength;* ε_f = *strain to failure;* ε_y = *yield strain;* N_f = *number of cycles to failure;* σ_{fat} = *fatigue strength;* E *loss = modulus degradation; OB = osteoblast; SBF = simulated body fluid; micro-CT = micro-computed tomography.*
[a]*Location: Nanyang Technological University, Singapore.*
[b]*Location: Friedrich-Alexander-University, Erlangen-Nuremberg, Erlangen, Germany.*
[c]*Location: University of Notre Dame, Notre Dame, IN, USA.*
[d]*Location: University of Hong Kong, Hong Kong.*
[e]*Location: Nagoya University, Nagoya, Japan.*

Table 11.2 Calcium Orthophosphate Reinforcements for Bioactive Polymer Composites

Ca/P	Abbreviation	Chemical Formula	Chemical Name	Mineral Name	$-\log (K_{sp})$[a]	Crystal Structure
0.50	MCPA	$Ca(H_2PO_4)_2$	Monocalcium phosphate, anhydrous		1.14 [36]	Triclinic
0.50	MCPM	$Ca(H_2PO_4)_2 \cdot H_2O$	Monocalcium phosphate monohydrate		1.14 [36]	Triclinic
1.0	DCPA	$CaHPO_4$	Dicalcium phosphate, anhydrous	Monetite	6.90 [37]	Triclinic
1.0	DCPD	$CaHPO_4 \cdot 2H_2O$	Dicalcium phosphate dihydrate	Brushite	6.59 [38]	Monoclinic
1.33	OCP	$Ca_8H_2(PO_4)_6 \cdot 5H_2O$	Octacalcium phosphate		96.6 [39]	Triclinic
1.15–1.5	ACP	$Ca_xH_y(PO_4)_z \cdot nH_2O$[b]	Amorphous calcium phosphate		25–28 [40]	Amorphous
1.5	α-TCP	α-$Ca_3(PO_4)_2$	α-Tricalcium phosphate		25.5 [41]	Monoclinic
1.5	β-TCP	β-$Ca_3(PO_4)_2$	β-Tricalcium phosphate	Whitlockite	28.9 [42]	Rhombohedral
1.5–1.67	cdHA	$Ca_{10-x}(HPO_4)_x(PO_4)_{6-x}(OH)_{2-x}$[c]	Calcium-deficient hydroxyapatite		~85.1 [43]	Hexagonal
1.67	HA, HAp	$Ca_{10}(PO_4)_6(OH)_2$	Calcium hydroxyapatite	Hydroxyapatite	116.8 [44]	Hexagonal
1.67	FAp	$Ca_{10}(PO_4)_6F_2$	Calcium fluoroapatite	Fluoroapatite	121.0 [45]	Hexagonal
~1.67	CO_3Ap	$Ca_{10}(PO_4)_6(OH)_{2-2x}(CO_3)_x$[d]	Carbonated hydroxyapatite	Dahllite	102.8 [46]	Hexagonal
2.0	TTCP, TetCP	$Ca_4(PO_4)_2O$	Tetracalcium phosphate	Hilgenstockite	38.0 [47]	Monoclinic

[a] *Measured or calculated at 25 °C.*
[b] $n = 3–4.5$.
[c] $0 < x < 1$.
[d] *A-type carbonate substitution for hydroxyls is shown. Carbonate may also substitute for phosphate (B-type). Therefore, a more general chemical formula for A- or B-type substitution is* $Ca_{10-2x/3}(PO_4)_{6-x}(CO_3)_x(OH)_{2-x/3}$.

with few crystalline defects and a relatively large crystal size, although the particle size may be tailored by grinding and/or sorting. Low-temperature synthesis ($\leq$200 °C)—including hydrothermal synthesis and precipitation—generally enables greater control over crystal defects (disorder), doping, size, and morphology. For example, calcium-deficient, carbonated, and other defective HA crystals prepared by low-temperature synthesis exhibit greater solubility than stoichiometric HA prepared by high-temperature synthesis (Table 11.2), which may lead to greater bioactivity [48]. Powders prepared by high-temperature solid-state reactions or calcination are generally equiaxed or spherical (Fig. 11.3). Single-crystal HA whiskers or platelets, which mimic the morphology of natural apatite crystals in mineralized tissues (Fig. 11.3), have been prepared by hydrothermal synthesis [49–51] and molten salt synthesis [52]. The size of hydrothermally synthesized HA has ranged from the extremes of nanoscale ($\leq$100 nm) [53] to several millimeters [54].

11.2.3 Composite Manufacturing and Microstructure

PAEK composites have been prepared by (1) compounding and injection molding [11–15,21], (2) cold pressing and pressureless sintering [19,20,33], (3) compression molding [25–32], and (4) selective laser sintering (SLS) [16–18,21–24] (Table 11.1). The latter three methods can also be used to produce macroporous PAEK scaffolds. Each method has its own advantages and disadvantages.

Compounding and injection molding is amenable to low-cost, high-volume commercial manufacturing of net shapes with a dense microstructure. Standard PAEK beads for injection molding may be used since bioactive reinforcements are mixed into the molten polymer by shear flow during compounding. However, the increased melt viscosity with the addition of calcium phosphate reinforcements limits reliable mixing and molding to less than 30–40 vol%, and high reinforcement fractions may cause equipment wear.

Cold pressing and pressureless sintering requires low overhead equipment costs and is amenable to almost any level of reinforcement during processing. Similarly, electrophoretic deposition and pressureless sintering was used to prepare uniform PEEK coatings reinforced by bioglass (45S5) particles [35]. The absence of applied pressure during sintering results in residual microporosity on the size scale of the starting powders. This microporosity may be beneficial for fluid entrapment and cell attachment, but is detrimental to mechanical properties [20].

Compression molding is similar to injection molding in relatively low-cost, high-volume commercial manufacturing of net shapes with a dense microstructure, except that productions rates are slightly lower and machining may be required to attain nongeometric shapes. Like cold pressing and pressureless sintering, compression molding is amenable to nearly any level of reinforcement during processing. However, unlike cold pressing and pressureless sintering, the resultant microstructure is fully dense, resulting in improved mechanical properties. Furthermore, tailored macroporosity has been

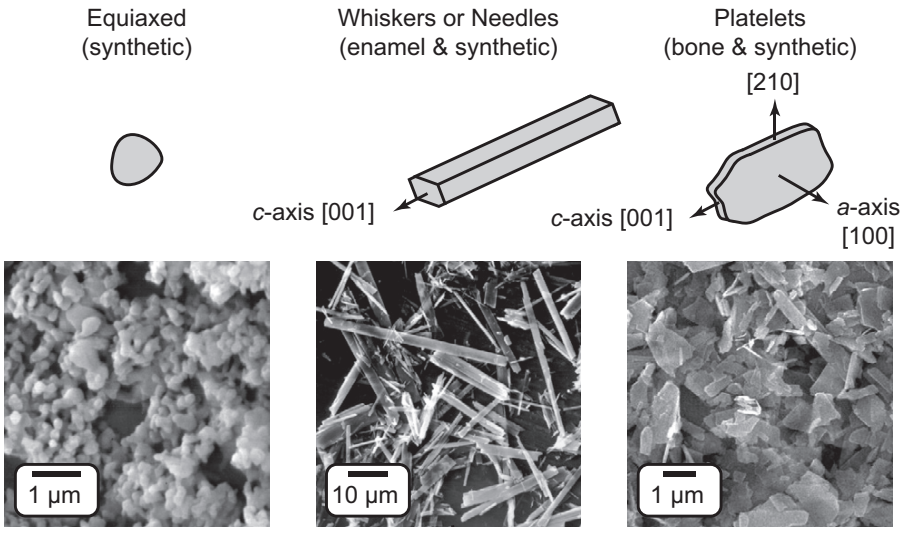

Figure 11.3 Schematic diagram (not to scale) showing common morphologies of natural and synthetic hydroxyapatite (HA) crystals. The SEM micrographs show equiaxed HA crystals prepared by calcination, as well as whisker and plate-like calcium-deficient HA crystals prepared by hydrothermal synthesis.

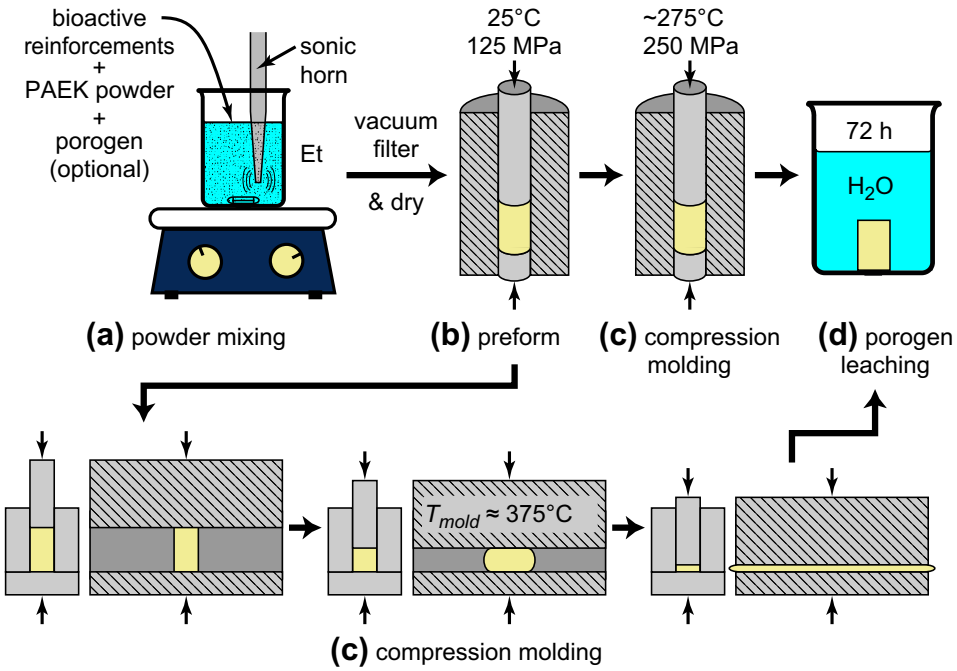

Figure 11.4 Schematic diagram showing compression molding as a flexible platform for the production of bioactive and porous PAEK composites of various size and shape. The process steps include (a) powder mixing in suspension and wet consolidation, (b) cold pressing a composite preform, (c) compression molding in dies designed for controlled flow and final shapes, and (d) leaching the porogen (if applicable).

produced by simply adding a porogen (e.g., sodium chloride) that is removed by soaking in a solvent after molding [28–30]. Thus, compression molding has been used as a flexible platform (Fig. 11.4) for the production of dense and/or macroporous bioactive PAEK composites of varying size and shape (Fig. 11.5).

SLS offers low overhead equipment costs and net shape manufacturing, especially for macroporous scaffolds with tailored architecture [18]. Customized objects can be fabricated directly from image files [computed tomography (CT) or computer-aided design (CAD)], but the process may be slow for commercial production. Also, the maximum reported porosity and reinforcement volume fraction has been limited to 70–74 vol% and 22 vol%, respectively [18], which was noted to be at least partly due to poor mechanical integrity [16,17]. Moreover, the porosity is dependent on the reinforcement content and laser power [18]. Finally, the presence of carbon black, which is added to aid particle flow in SLS, may not affect cytocompatibility [23] but could lead to undesirable blackening of adjacent tissue after long-term implantation.

The processing temperature and time is critical for each of the above methods. Excessive temperature and time can cause oxidation of PAEK polymers, while inadequate temperature and time can lead to poor densification and mechanical integrity. Increased melt temperature resulted in significantly decreased crystallinity in dense HA-reinforced PEEK (Victrex 450G) [11]. A recent investigation of HA-reinforced PEEK scaffolds showed that an increased mold temperature resulted in decreased crystallinity in high- and low-molecular-weight PEEK (Invibio LT1PF and LT3UF, respectively) [31].

Heat treatment may be necessary or advantageous following any of the above shape-forming processes in order to relieve residual shrinkage stress or tailor crystallinity. An annealing treatment above the glass transition temperature of PEEK (143 °C) has been shown to be beneficial for some mechanical properties and the homogeneity of HA-reinforced PEEK [13,25]. This effect was presumably due to relieving residual stress and controlling recrystallization although the crystallinity was not measured. In as-molded composites, the measured crystallinity of PEEK ranged from 22% to 31% and exhibited little or no change with increased levels of HA reinforcement [11,34]. However, further investigation revealed that PEEK crystallinity in the outermost "skin" of composites

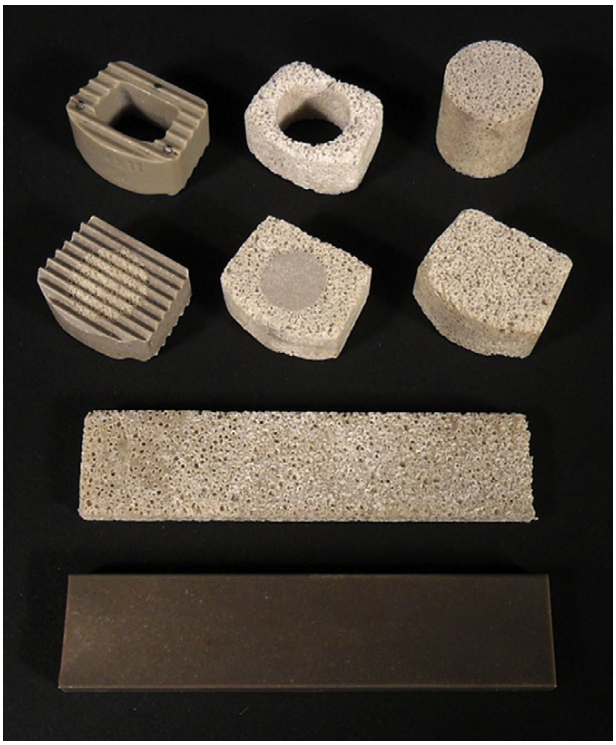

Figure 11.5 Photograph showing various examples of dense and/or macroporous bioactive PAEK composites of varying size and shape produced by compression molding, compared with a commercial cervical spinal fusion cage (upper left). All specimens comprised PEEK (Invibio LT1) reinforced with 20 vol% calcium-deficient HA whiskers and were molded either fully dense or with 75 vol% porosity using a sodium chloride porogen (Fig. 11.4). Note that the dense beam at the bottom has dimensions of 43 × 10 × 2.5 mm.

was unaffected (20–22%), but crystallinity in the bulk "core" region of composites increased from 24% to 31% with 0 to 40 vol% HA reinforcement [12]. Differences in the core/skin are not unexpected due to differences in cooling rate and were subsequently minimized by the aforementioned annealing treatments. There has been little investigation of the effects of the cooling rate or annealing treatment on the crystallinity of calcium phosphate-reinforced PEEK composites, as well as the presence or effects of an interphase layer adjacent to reinforcement particles. This is surprising considering their known importance in carbon fiber-reinforced PEEK [55].

Bioactive PAEK composites have been machined after shape-forming processes using standard tooling. Porous scaffolds were also readily machined prior to leaching the porogen [30], as shown by grooves milled onto the top surface of an implant shown in Fig. 11.5.

Quantitative microstructural characterization has mainly included the apparent density of the composite, the PAEK crystallinity (above), and the size and volume fraction of the bioactive reinforcements. If the PAEK polymer can be pyrolized at a temperature where the bioactive reinforcements are unaffected, the size, morphology, and volume fraction of reinforcements in the composite can be measured after shape forming [12,26,56]. Dispersion of the reinforcements in the PAEK matrix and failure surfaces has been typically assessed qualitatively from optical or SEM micrographs. The exposure of bioactive reinforcements on PAEK surfaces has been qualitatively observed from SEM micrographs and von Kossa staining [28]. Note that the broad fluorescence emission spectrum of PEEK, ranging from 400 to 600 nm [57], interferes with common fluorophores (e.g., alizarin, calcein) for labeling calcium. The crystallographic and morphological orientation of single-crystal HA whisker reinforcements in PEEK was characterized using quantitative texture analysis with X-ray diffraction (XRD) [25]. Composites exhibited a mechanically advantageous preferred orientation of HA whiskers along the length of compression-molded tensile bars, which was similar to that exhibited by apatite crystals in human cortical bone tissue along the principal stress direction. The pore volume, architecture, and interconnectivity of HA whisker-reinforced PEKK scaffolds were quantitatively characterized using micro-CT [28].

There is a need for greater attention to quantitative microstructural characterization in order to establish structure–property relationships and rationally design bioactive PAEK composites. A "make it and break it" approach (processing–properties) that does not pay careful attention to the composite microstructure [10] will be detrimental to continued progress.

11.3 Structure–Property Relationships

11.3.1 Biological Properties

PAEK polymers are well known to be biocompatible and bioinert [2,3,58–64]. PAEK and carbon fiber-reinforced PAEK were encapsulated by a layer of fibrous tissue in vivo after intramuscular implantation in rabbits [58,60], subcutaneous implantation in sheep [63], fixation of a canine femoral osteotomy [60], and injection of particles into the spinal canal of

rabbits [62]. PAEK and carbon fiber-reinforced PAEK were only partially encapsulated by fibrous tissue in interbody spinal fusion of sheep [2] and goats [61], although these implants were augmented with osteoinductive autograft or rhBMP-2. Retrievals for failed spinal fusion cages in humans exhibited no direct bone apposition to carbon fiber-reinforced PAEK implants [65].

Calcium phosphates, on the other hand, are well known to be biocompatible and bioactive [48,66−68]. Bioactivity is the ability of a biomaterial to elicit or modulate a favorable response ("activity") from any part of a biological organism [10]. Calcium phosphates consistently exhibit direct apposition of bone tissue, without the use of autograft or BMPs, no matter whether implanted in osseous defects [48,67] or non-osseous sites [68−70]. In the latter case of subcutaneous or intramuscular implantation, HA may be considered osteoinductive. The bioactivity of calcium phosphates in vivo has been attributed to the release of calcium by dissolution and/or osteoclastic resorption, as well as an affinity for binding osteoinductive proteins from the implant site [66,68].

Therefore, a key consideration in the choice of bioactive phases is the solubility product (K_{sp}), which can vary widely (Table 11.2). Solubility may aid bioactivity through calcium release and cellular signaling, but may also lead to complete degradation of bioactive reinforcements. Degradation of reinforcements may be desirable in the case of degradable polymer composites. However, PAEK polymers are not degradable and thus PAEK composites are intended to perform as permanent implants. Therefore, the complete degradation of bioactive reinforcements in PAEK composites could lead to a loss of biological and/or mechanical function. After 86 weeks in a minipig trabecular bone defect, 97% of a β-TCP bone substitute was completely removed [71]. This suggests that for long-term function, bioactive reinforcements in PAEK composites should comprise HA, calcium-deficient HA, carbonated HA, or doped HA. The solubility and bioactivity of HA are generally increased with increased defects in the crystal structure, including ionic substitutions, and decreased particle size [48,68,72].

Investigations of HA-reinforced PAEK composites to date have mainly focused on in vitro assessment of bioactivity and cytocompatibility (Table 11.1). After immersion in simulated body fluid (SBF), a layer of carbonated apatite was deposited on HA reinforcements, but not the PEEK matrix, confirming that the HA reinforcements were bioactive and the PEEK matrix was bioinert [18,19,32]. The thickness and surface coverage of the apatite layer increased with increased HA [19,32] or calcium silicate [33] content, as well as for strontium-substituted HA compared with HA [32]. In order to avoid interference from the bioactive reinforcements in the underlying composite, the apatite layer should be removed from the composite surface for characterization using XRD, Fourier transform infrared spectroscopy (FT-IR), and other surface analytical techniques [19].

Cell attachment on bioactive PAEK composites has been demonstrated using fibroblasts [18], human osteoblasts [21,32], and human fetal osteoblasts [22,23]. Osteoblast proliferation and spreading were reported to be greatest for bioglass (45S5)-reinforced PEEK, followed by PEEK and then β-TCP-reinforced PEEK [21−23]. However, another study reported no differences in osteoblast proliferation and alkaline phosphatase activity (differentiation) for PEEK, HA-reinforced PEEK, and Sr-HA-reinforced PEEK [32]. HA alone is known to suppress cell proliferation but enhance differentiation [73]. Little attention seems to have been given to the broad fluorescence emission spectrum of PEEK, ranging from 400 to 600 nm [57], and possible interference with common fluorophores (e.g., alizarin, calcein, fluorescein isothiocyanate, rhodamine) used for labeling proteins and mineralization. For example, increased bioactive reinforcement content could lead to increased fluorescence from a biochemical assay with concomitant decreased fluorescence from the PAEK matrix. Systematic investigations for the effects of the bioactive reinforcement composition, content, size, and morphology on cellular behavior are needed in the future.

There is currently a paucity of data for the in vivo osteoconductivity or osteointegration of bioactive PAEK composites. An early study reported bone ingrowth into a porous HA-reinforced PEEK scaffold prepared by SLS at 16 weeks postimplantation in pigs [16], but no further details were provided. More recently, PEEK reinforced with 4 vol% β-TCP prepared by SLS was implanted into 10-mm-diameter cranial defects in pigs [24]. The thickness of the fibrous tissue layer encapsulating the implant decreased with increased β-TCP content and time postimplantation. At 24 weeks postimplantation, there was direct apposition of bone to β-TCP reinforcements but not the PEEK matrix. Moreover, the

push-out strength of β-TCP-reinforced PEEK implants was 13% greater than that for PEEK alone [24].

11.3.2 Functional Properties

A number of other functional properties are of importance to bioactive PAEK composites. Dense PAEK composites could conceivably be shaped intraoperatively using a high-speed burr, whereas porous PAEK composites could be shaped intraoperatively using a scalpel or rongeur. The pore architecture and interconnectivity of PAEK composite scaffolds has been quantitatively characterized using segmented micro-CT images [28], but there have been no experimental or computational measurements of permeability to date. Calcium phosphate reinforcement does not detract from the advantageous radiolucency of PAEK, but may be used instead of barium sulfate to tailor the radiopacity for visualization of an implant by X-ray imaging. For example, PAEK reinforced with 40–50 vol% HA exhibits X-ray attenuation similar to human cortical bone. Finally, just as the greater cost of PAEK polymers over conventional biomedical thermoplastics (e.g., polyethylene) had to be justified by enhanced performance, the added cost of raw materials and manufacturing bioactive PAEK composites will have to be justified by additional performance benefits in order to reach the market.

11.3.3 Mechanical Properties

The mechanical properties of bioactive PAEK composites have been evaluated by static uniaxial tension [12–14,20,21,25], cyclic uniaxial tension [14,15], static uniaxial compression [20,29–31], implant push-out strength [24], ultrasonic wave propagation [25,26], static four-point bending [32], cyclic four-point bending [27], static three-point bending [33], and micromechanical models [26,74,75]. PAEK composites have exhibited excellent static mechanical properties and fatigue properties compared with other polymers with bioactive reinforcements (Fig. 11.6). Both dense and porous PAEK composites have been engineered to mimic mechanical properties exhibited by human cortical and trabecular bone tissue, respectively (Table 11.3).

Dense HA-reinforced PEEK was able to mimic the longitudinal elastic modulus of human cortical bone at a similar volume fraction of HA [12–14,25]

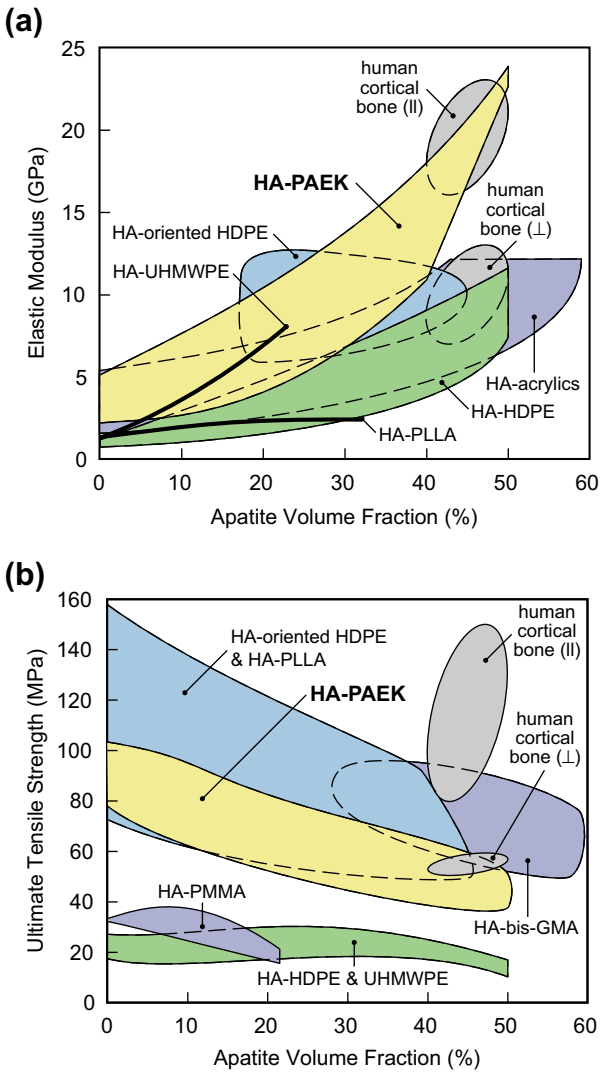

Figure 11.6 The elastic modulus (a) and ultimate tensile strength (b) of human cortical bone tissue compared to polymers reinforced with varying amounts of HA. The mechanical properties of cortical bone are shown for loading parallel (||) and perpendicular (⊥) to the longitudinal anatomic axis. Note that the regions are shown to simplify and be inclusive of a large number of data points from the literature for high-density polyethylene (HDPE) [6,8,76], PAEK [13–15,21,25], ultrahigh-molecular-weight polyethylene (UHMWPE) [77], acrylics—including polymethyl methacrylate (PMMA) [78–80] and bisphenol-*a*-glycidyl methacrylate/triethylene glycol dimethacrylate (bis-GMA/TEG-DMA) [81–84]—PLLA [85,86], and anisotropic (oriented) HDPE [87–90]. The dataset was limited to uniaxial tensile tests in order to be free from ambiguity due to variations in testing methods (e.g., bending tests).

Table 11.3 Dense HA-Reinforced PAEK Composites have Exhibited an Elastic Modulus (*E*) and Ultimate Tensile Strength (UTS) Similar to that of Human Cortical Bone Tissue, Porous HA Whisker-Reinforced PEKK Scaffolds have Exhibited an Apparent Compressive Elastic Modulus (*E*) and Yield Strength (YS) Similar to that of Human Vertebral Trabecular Bone.

Uniaxial Tension	**Porosity (%)**	**Apatite Content (vol%)**	***E* (GPa)**	**UTS (MPa)**
Dense HA powder and whisker-reinforced PAEK [12–14,25]	~0	0–40	3–19	25–118
Human cortical bone (longitudinal) [91,92]	~5–10	~40	16–23	80–150
Uniaxial Compression			***E* (MPa)**	**YS (MPa)**
Porous HA whisker-reinforced PAEK [29–31]	75–90	0–40	1–190	0.002–2.7
Human vertebral trabecular bone [93,94]	~80–95	~40	20–500	0.5–4

(Table 11.3), whereas all other polymers with bioactive reinforcements were only able to mimic the transverse elastic modulus of human cortical bone (Fig. 11.6a). The elastic modulus was increased with increased reinforcement, as expected. HA-reinforced PEEK was able to achieve the transverse ultimate tensile strength of human cortical bone at a similar volume fraction of HA [12–14,25], similar to other polymers, and reached the low end of the longitudinal ultimate tensile strength of human cortical bone at lower levels of HA reinforcement (Fig. 11.6b). The ultimate tensile strength was decreased with increased reinforcement for all HA-reinforced polymers. HA reinforcements act as flaws in the polymer matrices due to limited interfacial bonding. Therefore, a design tradeoff exists between increased bioactivity, but decreased strength, with increased levels of calcium phosphate reinforcement. The tradeoff can be lessened by improving load transfer from the matrix to reinforcement.

The use of single-crystal HA whiskers was previously shown to result in significantly improved tensile and fatigue properties when directly compared with conventional, equiaxed HA powder reinforcements in HDPE composites [76,95]. Compression-molded HA whisker-reinforced PEEK (Victrex 150XF) [25] exhibited a greater elastic modulus and ultimate tensile strength compared with injection-molded HA powder-reinforced PEEK (Victrex 450G) [12–14]. The difference in PEEK molecular weight was opposite to the difference in mechanical properties; therefore, this difference was most likely due to the HA reinforcement morphology, but may have also been influenced by differences in PEEK crystallinity. HA whisker-reinforced PEEK composites were orthotropic [25,26] due to a preferred orientation of the HA whiskers in the direction of flow during molding in a channel die (Fig. 11.4). The degree of preferred orientation and anisotropy were tailored to be similar to human cortical bone [25] and were strongly correlated [26].

Micromechanical models have been used to study the effects of the PEEK/HA interface on the composite mechanical properties [74,75], and the effects of the reinforcement morphology and orientation on anisotropic elastic constants [26]. Once validated against experimental data, micromechanical models can be useful for designing new bioactive PAEK composites for improved performance and elucidating the mechanisms underlying structure–property relationships.

In tension–tension fatigue, injection-molded HA-powder-reinforced PEEK exhibited a fatigue strength at 1 million cycles of approximately 60, 40, 35, and 30 MPa for 0, 10, 20, and 30 vol% HA, respectively [14,15]. These loads were typically at least 50% of the ultimate tensile strength. Composites failed by debonding of the HA/PEEK interface, followed by initiation and growth of microcracks that

accumulated to form a fatigue crack [15]. The residual elastic modulus and ultimate tensile strength following fatigue to 1 million cycles was 5−30% and 15−15%, respectively, for 0−30 vol% HA [15]. In four-point bending fatigue, compression-molded HA-whisker-reinforced PEKK exhibited a fatigue strength at 2 million cycles of approximately 75, 60, and 40 MPa for 0, 20, and 40 vol% HA whiskers, respectively [27]. Figure 11.7 shows a representative fatigue failure surface of PEKK reinforced with 20 vol% HA whiskers.

Finally, porous PEKK [29,30] and PEEK [31] scaffolds were prepared by compression molding and porogen leaching (Fig. 11.4) with 75−90 vol% porosity and 0−40 vol% HA whisker reinforcements. Increased porosity resulted in a nonlinear decrease in the elastic modulus and yield strength, as expected. The mechanical properties were generally maximum and most reliable at 20 vol% HA reinforcement. The compressive modulus, yield strength, and yield strain increased with increased mold temperature [29,31] to a maximum at ~375−385 °C due to improved densification [31]. PEKK scaffolds with 75% porosity and 20 vol% HA molded at 375 °C exhibited a mean compressive modulus and yield strength of 149 and 2.2 MPa, respectively, which was the highest of the conditions investigated and similar to human vertebral trabecular bone (Table 11.3). The mechanical properties of porous calcium phosphate-reinforced PAEK produced by SLS have not been reported.

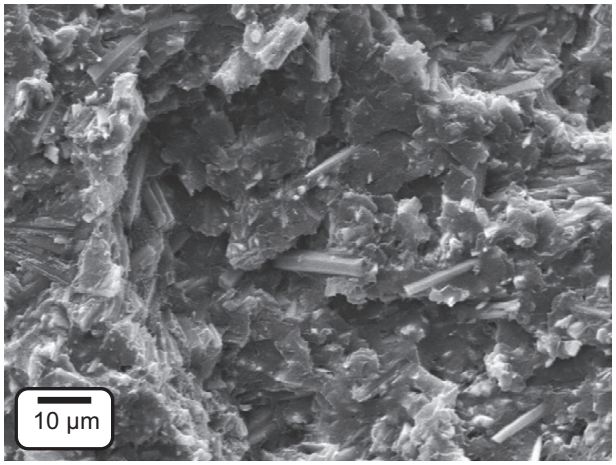

Figure 11.7 SEM micrograph showing a representative failure surface for PEKK (OXPEKK-C) reinforced with 20 vol% HA whiskers after loading in cyclic four-point bending fatigue. HA whiskers are visible embedded or protruding from the PEKK matrix.

11.4 Concluding Remarks

This chapter reviewed key results and accomplishments from the first decade of work on bioactive PAEK composites, and did so within the framework of processing−structure−property relationships. With only a little more than one decade of active work largely centered in three research groups located in three continents (Table 11.1), this chapter is far from finished. Key processing−structure−property relationships in bioactive PAEK composites are only beginning to be established. Documented research efforts for bioactive PAEK composites began with one article published in 1999 [11]. In 2009, six papers were published on bioactive PAEK composites. Therefore, research and development of bioactive PAEK composites promises to be an active area of continued growth for the foreseeable future. This growth will be driven by potential clinical applications, including permanent implant fixation (e.g., interbody spinal fusion), synthetic bone graft substitutes, and fracture fixation hardware (screws, plates, rods, etc.), among others. Moreover, the limited supply and risks associated with autograft and allograft tissue, combined with the cost and recent scrutiny by the FDA for the use of rhBMP-2 in cervical spinal fusion [96], should provide ample clinical and commercial motivation for continued research and development of bioactive PAEK composites.

Numerous gaps in the current state of knowledge for bioactive PAEK composites were noted throughout this chapter. Foremost among these is a need for in vivo investigations on the osteointegration of bioactive PAEK composites. Continued materials engineering of processing methods and microstructures for optimized mechanical properties should result in dense and porous bioactive PAEK composites that meet or exceed the mechanical properties of cortical and cancellous, respectively, allografts and autografts. A major goal for the next decade of work should be translation to commercial products that address clinical needs.

References

[1] S.L. Evans, P.J. Gregson, Composite technology in load-bearing orthopaedic implants, Biomaterials 19 (15) (1998) 1329−1342.
[2] J.M. Toth, M. Wang, B.T. Estes, J.L. Scifert, H.B. Seim, A.S. Turner, Polyetheretherketone

as a biomaterial for spinal applications, Biomaterials 27 (2006) 324−334.
[3] S.M. Kurtz, J.N. Devine, PEEK biomaterials in trauma, orthopedic, and spinal implants, Biomaterials 28 (2007) 4845−4869.
[4] R.K. Roeder, G.L. Converse, R.J. Kane, W. Yue, Hydroxyapatite reinforced polymer biocomposites for synthetic bone substitutes, JOM 60 (3) (2008) 38−45.
[5] K. Rezwan, Q.Z. Chen, J.J. Blaker, A.R. Boccaccini, Biodegradable and bioactive porous polymer/inorganic composite scaffolds for bone tissue engineering, Biomaterials 27 (2006) 3413−3431.
[6] W. Bonfield, M.D. Grynpas, A.E. Tully, J. Bowman, J. Abram, Hydroxyapatite reinforced polyethylene—a mechanically compatible implant material for bone replacement, Biomaterials 2 (1981) 185−186.
[7] K.E. Tanner, R.N. Downes, W. Bonfield, Clinical applications of hydroxyapatite reinforced materials, Brit. Ceram. Trans. 93 (3) (1994) 104−107.
[8] M. Wang, R. Joseph, W. Bonfield, Hydroxyapatite−polyethylene composites for bone substitution: effects of ceramic particle size and morphology, Biomaterials 19 (24) (1998) 2357−2366.
[9] L.D. Silvio, M.J. Dalby, W. Bonfield, Osteoblast behaviour on HAP/PE composite surfaces with different HA volumes, Biomaterials 23 (2002) 101−107.
[10] R.K. Roeder, A paradigm for the integration of biology in materials science and engineering, JOM 62 (7) (2010) 49−55.
[11] M.S. Abu Bakar, P. Cheang, K.A. Khor, Thermal processing of hydroxyapatite reinforced polyetheretherketone composites, J. Mater. Proc. Technol. 89−90 (1999) 462−466.
[12] M.S. Abu Bakar, P. Cheang, K.A. Khor, Tensile properties and microstructural analysis of spheroidized hydroxyapatite−poly (ether-etherketone) biocomposites, Mater. Sci. Eng. A345 (13) (2003) 55−63.
[13] M.S. Abu Bakar, P. Cheang, K.A. Khor, Mechanical properties of injection molded hydroxyapatite−polyetheretherketone biocomposites, Compos. Sci. Technol. 63 (2003) 421−425.
[14] M.S. Abu Bakar, M.H.W. Cheng, S.M. Tang, S.C. Yu, K. Liao, C.T. Tan, et al., Tensile properties, tension−tension fatigue and biological response of polyetheretherketone−hydroxyapatite composites for load-bearing orthopedic implants, Biomaterials 24 (13) (2003) 2245−2250.
[15] S.M. Tang, P. Cheang, M.S. Abu Bakar, K.A. Khor, K. Liao, Tension−tension fatigue behavior of hydroxyapatite reinforced polyetheretherketone composites, Int. J. Fatigue 26 (2004) 49−57.
[16] K.H. Tan, C.K. Chua, K.F. Leong, C.M. Cheah, P. Cheang, M.S. Abu Bakar, et al., Scaffold development using selective laser sintering of polyetheretherketone−hydroxyapatite biocomposite blends, Biomaterials 24 (2003) 3115−3123.
[17] K.H. Tan, C.K. Chua, K.F. Leong, C.M. Cheah, W.S. Gui, W.S. Tan, et al., Selective laser sintering of biocompatible polymers for applications in tissue engineering, Biomed. Mater. Eng. 15 (2005) 113−124.
[18] K.H. Tan, C.K. Chua, K.F. Leong, M.W. Naing, C.M. Cheah, Fabrication and characterization of three-dimensional poly(ether-ether-ketone)/hydroxyapatite biocomposite scaffolds using laser sintering, J. Eng. Med. 219 (2005) 183−194.
[19] S. Yu, K.P. Hariram, R. Kumar, P. Cheang, K.K. Aik, In vitro apatite formation and its growth kinetics on hydroxyapatite/polyetheretherketone biocomposites, Biomaterials 26 (2005) 2343−2352.
[20] C. Hengky, B. Kelsen, Saraswati, P. Cheang, Mechanical and biological characterization of pressureless sintered hydroxyapatite−polyetheretherketone biocomposite, International Conference on Biomedical Engineering (ICBME) Proceedings 23 (2009) 261−264.
[21] L. Petrovic, D. Pohle, H. Münstedt, T. Rechtenwald, K.A. Shlegel, S. Rupprecht, Effect of βTCP filled polyetheretherketone on osteoblast cell proliferation in vitro, J. Biomed. Sci. 13 (2006) 41−46.
[22] D. Pohle, S. Ponader, T. Rechtenwald, M. Schmidt, K.A. Shlegel, H. Münstedt, et al., Processing of three-dimensional laser sintered polyetheretherketone composites and testing of osteoblast proliferation in vitro, Macromol. Symp. 253 (2007) 65−70.

[23] C. von Wilmowsky, E. Vairaktaris, D. Pohle, T. Rechtenwald, R. Lutz, H. Münstedt, et al., Effects of bioactive glass and β-TCP containing three-dimensional laser sintered polyetheretherketone composites on osteoblasts in vitro, J. Biomed. Mater. Res. 87A (2008) 896−902.

[24] C. von Wilmowsky, R. Lutz, U. Meisel, S. Srour, S. Rupprecht, T. Toyoshima, et al., In vivo evaluation of β-TCP containing 3D laser sintered poly(ether ether ketone) composites in pigs, J. Bioactive Compatible Polym. 24 (2009) 169−184.

[25] G.L. Converse, W. Yue, R.K. Roeder, Processing and tensile properties of hydroxyapatite-whisker-reinforced polyetheretherketone, Biomaterials 28 (6) (2007) 927−935.

[26] J.M. Deuerling, J.S. Vitter, G.L. Converse, R.K. Roeder. Prediction of orthotropic elastic constants in hydroxyapatite whisker reinforced polyetheretherketone composites using orientation distribution functions. J. Eng. Mater. Technol., in press.

[27] G.L. Converse, T.L. Conrad, R.K. Roeder, Fatigue life of hydroxyapatite whisker reinforced polyetherketoneketone, Trans. Soc. Biomaterials 32 (2009) 584.

[28] G.L. Converse, T.L. Conrad, C.H. Merrill, R.K. Roeder, Hydroxyapatite whisker-reinforced polyetherketoneketone bone ingrowth scaffolds, Acta Biomater. 6 (3) (2010) 856−863.

[29] G.L. Converse, T.L. Conrad, R.K. Roeder, Mechanical properties of hydroxyapatite whisker reinforced polyetherketoneketone composite scaffolds, J. Mech. Behav. Biomed. Mater. 2 (6) (2009) 627−635.

[30] R.K. Roeder, S.M. Smith, T.L. Conrad, N.J. Yanchak, C.H. Merrill, G.L. Converse, Porous and bioactive PEEK implants for interbody spinal fusion, Adv. Mater. Processes 167 (10) (2009) 46−48.

[31] T.L. Conrad, D.D. Jaekel, S.M. Kurtz, R.K. Roeder, Unpublished results.

[32] K.L. Wong, C.T. Wong, W.C. Liu, H.B. Pan, M.K. Fong, W.M. Lam, et al., Mechanical properties and in vitro response of strontium-containing hydroxyapatite/polyetheretherketone composites, Biomaterials 30 (2009) 3810−3817.

[33] I.Y. Kim, A. Sugino, K. Kikuta, C. Ohtsuki, S.B. Cho, Bioactive composites consisting of PEEK and calcium silicate powders, J. Biomater. Appl. 24 (2009) 105−118.

[34] B.J. Meenan, C. McClorey, M. Akay, Thermal analysis studies of poly(etheretherketone)/hydroxyapatite biocomposite mixtures, J. Mater. Sci. Mater. Med. 11 (2000) 481−489.

[35] A.R. Boccaccini, C. Peters, J.A. Roether, D. Eifler, S.K. Misra, E.J. Minay, Electrophoretic deposition of polyetheretherketone (PEEK) and PEEK/bioglass® coatings on NiTi shape memory alloy wires, J. Mater. Sci. 41 (2006) 8152−8159.

[36] J.C. Elliott, Structure and Chemistry of the Apatites and Other Calcium Orthophosphates, Elsevier Science B.V., Amsterdam, 1994.

[37] H. McDowell, W.E. Brown, J.R. Sutter, Solubility study of calcium hydrogen phosphate: ion pair formation, Inorg. Chem. 10 (1971) 1638−1643.

[38] T.M. Gregory, E.C. Moreno, W.E. Brown, Solubility of $CaHPO_4 \cdot 2H_2O$ in the system $Ca(OH)_2-H_3PO_4-H_2O$ at 5, 15, 25 and 37.5 °C, J. Res. Nat. Bur. Stand. 74A (1970) 461−475.

[39] M.S. Tung, N. Eidelman, B. Sieck, W.E. Brown, Octacalcium phosphate solubility product from 4 to 37 °C, J. Res. Nat. Bur. Stand. 93 (1988) 613−624.

[40] M.R. Christoffersen, J. Christoffersen, W. Kibalczyc, Apparent solubilities of two amorphous calcium phosphates and of octacalcium phosphate in the temperature range 30−42 °C, J. Cryst. Growth 106 (1990) 349−354.

[41] B.O. Fowler, S. Kuroda, Changes in heated and in laser-irradiated human tooth enamel and their effects on solubility, Calcif. Tissue Int. 38 (1986) 197−208.

[42] T.M. Gregory, E.C. Moreno, J.M. Patel, W.E. Brown, Solubility of β-$Ca_3(PO_4)_2$ in the system $Ca(OH)_2-H_3PO_4-H_2O$ at 5, 15, 25 and 37 °C, J. Res. Nat. Bur. Stand. 78A (1974) 667−674.

[43] F.C.M. Driessens, R.M.H. Verbeeck, Biominerals, CRC Press, Boca Raton, 1990.

[44] H. McDowell, T.M. Gregory, W.E. Brown, Solubility of $Ca_5(PO_4)_3OH$ in the system $Ca(OH)_2-H_3PO_4-H_2O$ at 5, 15, 25, and 37 °C, J. Res. Nat. Bur. Stand. 81A (1977) 273−281.

[45] J.C. Moreno, M. Kresak, R.T. Zahradnik, Physiochemical aspects of fluoride−apatite

systems relevant to the study of dental caries, Caries Res. 11 (Suppl. 1) (1977) 142−171.
[46] A. Ito, K. Maekawa, S. Tsutsumi, F. Ikazaki, T. Tateishi, Solubility product of OH-carbonated hydroxyapatite, J. Biomed. Mater. Res. 36A (1997) 522−528.
[47] S. Matsuya, S. Takagi, L.C. Chow, Hydrolysis of tetracalcium phosphate in H_3PO_4 and KH_2PO_4, J. Mater. Sci. 31 (1996) 3263−3269.
[48] T. Okuda, K. Ioku, I. Yonezawa, H. Minagi, Y. Gonda, G. Kawachi, et al., The slow resorption with replacement of bone by a hydrothermally synthesized pure calcium-deficient hydroxyapatite, Biomaterials 29 (2008) 2719−2728.
[49] W. Suchanek, H. Sada, M. Yashimi, M. Kakihana, M. Yoshimura, Biocompatible whiskers with controlled morphology and stoichiometry, J. Mater. Res. 10 (3) (1995) 521−529.
[50] R.K. Roeder, G.L. Converse, H. Leng, W. Yue, Kinetic effects on hydroxyapatite whiskers synthesized by the chelate decomposition method, J. Am. Ceram. Soc. 89 (7) (2006) 2096−2104.
[51] I.S. Neira, Y.V. Kolen'ko, O.I. Lebedev, G.V. Tendeloo, H.S. Gupta, F. Guitián, et al., An effective morphology control of hydroxyapatite crystals via hydrothermal synthesis, Cryst. Growth Des. 9 (1) (2009) 466−474.
[52] A.C. Tas, Molten salt synthesis of calcium hydroxyapatite whiskers, J. Am. Ceram. Soc. 84 (2) (2001) 295−300.
[53] L. Yubao, K. de Groot, J. de Wijn, C.P.A.T. Klein, S.V.D. Meer, Morphology and composition of nanograde calcium phosphate needle-like crystals formed by simple hydrothermal treatment, J. Mater. Sci. Mater. Med. 5 (6−7) (1994) 326−331.
[54] K. Teraoka, A. Ito, K. Onuma, T. Tateishi, S. Tsutsumi, Hydrothermal growth of hydroxyapatite single crystals under natural convection, J. Mater. Res. 14 (6) (1999) 2655−2661.
[55] S.-L. Gao, K. Kim J, Cooling rate influences in carbon fibre/PEEK composites. Part 1. Crystallinity and interface adhesion, Composites 31A (2000) 517−530.
[56] W. Yue, R.K. Roeder, Micromechanical model for hydroxyapatite whisker reinforced polymer biocomposites, J. Mater. Res. 21 (8) (2006) 2136−2145.
[57] H.-J. Cha, C.W. Frank, Annealing study of poly(ether ether ketone): temperature effect on molecular conformation and crystallinity, Korea Polym. J. 7 (3) (1999) 141−149.
[58] D.F. Williams, A. McNamara, R.M. Turner, Potential of polyetheretherketone (PEEK) and carbon-fibre-reinforced PEEK in medical applications, J. Mater. Sci. Lett. 6 (1987) 188−190.
[59] L.M. Wenz, K. Merrit, S.A. Brown, A. Moet, A.D. Steffee, In vitro biocompatibility of polyetheretherketone and polysulfone composites, J. Biomed. Mater. Res. 24 (1990) 207−215.
[60] K.A. Jockisch, S.A. Brown, T.W. Bauer, K. Merritt, Biological response to chopped-carbon-fiber-reinforced PEEK, J. Biomed. Mater. Res. 26 (1992) 133−146.
[61] J.W. Brantigan, P.C. McAfee, B.W. Cunningham, H. Wang, C.M. Orbegoso, Interbody lumbar fusion using a carbon fiber cage implant versus allograft bone, Spine 19 (13) (1994) 1436−1444.
[62] C.-H. Rivard, S. Rhalmi, C. Coillard, In vivo biocompatibility testing of PEEK polymer for a spinal implant system: a study in rabbits, J. Biomed. Mater. Res. 62 (4) (2002) 488−498.
[63] T. Nieminen, I. Kallela, E. Wuolijoki, H. Kainulainen, I. Hiidenheimo, I. Rantala, Amorphous and crystalline polyetheretherketone: mechanical properties and tissue reactions during a 3-year follow-up, J. Biomed. Mater. Res. 84A (2008) 377−383.
[64] K.B. Sagomonyants, M.L. Jarman-Smith, J.N. Devine, M.S. Aronow, G.A. Gronowicz, The in vitro response of human osteoblasts to polyetheretherketone (PEEK) substrates compared to commercially pure titanium, Biomaterials 29 (2008) 1563−1572.
[65] D. Togawa, T.W. Bauer, I.H. Leiberman, H. Sakai, Lumbar intervertebral body fusion cages: histological evaluation of clinically failed cages retrieved from humans, J. Bone Joint Surg. Am. 86 (2004) 70−79.
[66] L.L. Hench, Bioceramics: from concept to clinic, J. Am. Ceram. Soc. 74 (7) (1991) 1487−1510.

[67] H. Oguchi, K. Ishikawa, K. Mizoue, K. Seto, G. Eguchi, Long-term histological evaluation of hydroxyapatite ceramics in humans, Biomaterials 16 (1995) 33−38.
[68] R.Z. LeGeros, Properties of osteoconductive biomaterials: calcium phosphates, Clin. Orthop. Rel. Res. (395) (2002) 81−98.
[69] U. Ripamonti, Osteoinduction in porous hydroxyapatite implanted in heterotopic sites of different animal models, Biomaterials 17 (1996) 31−35.
[70] A.K. Gosain, L. Song, P. Riordan, M.T. Amarante, P.G. Nagy, C.R. Wilson, et al., A 1-year study of osteoinduction in hydroxyapatite-derived biomaterials in an adult sheep model: part I, Plast. Reconstr. Surg. 106 (2002) 619−630.
[71] J. Wiltfang, H.A. Merten, K.A. Schlegel, S. Schultze-Mosgau, F.R. Kloss, S. Rupprecht, et al., Degradation characteristics of α and β tri-calcium-phosphate (TCP) in minipigs, J. Biomed. Mater. Res. 63B (2002) 115−121.
[72] N. Patel, S.M. Best, W. Bonfield, I.R. Gibson, K.A. Hing, E. Damien, et al., A comparative study on the in vivo behavior of hydroxyapatite and silicon substituted hydroxyapatite granules, J. Mater. Sci. Mater. Med. 13 (2002) 1199−1206.
[73] R. Shu, R. McMullen, M.J. Baumann, L.R. McCabe, Hydroxyapatite accelerates differentiation and suppresses growth of MC3T3-E1 osteoblasts, J. Biomed. Mater. Res. 67A (4) (2003) 1196−1204.
[74] J.P. Fan, C.P. Tsui, C.Y. Tang, Modeling of the mechanical behavior of HA/PEEK biocomposite under quasi-static tensile load, Mater. Sci. Eng. A382 (2004) 341−350.
[75] J.P. Fan, C.P. Tsui, C.Y. Tang, C.L. Chow, Influence of interphase layer on the overall elasto-plastic behaviors of HA/PEEK biocomposite, Biomaterials 25 (2004) 5363−5373.
[76] R.K. Roeder, M.S. Sproul, C.H. Turner, Hydroxyapatite whiskers provide improved mechanical properties in reinforced polymer composites, J. Biomed. Mater. Res. 67A (3) (2003) 801−812.
[77] L. Fang, Y. Leng, P. Gao, Processing and mechanical properties of HA/UHMWPE nanocomposites, Biomaterials 27 (2006) 3701−3707.
[78] M.E. Islas-Blancas, J.M. Cervantes-Uc, R. Vargas-Coronado, J.V. Cauich-Rodríguez, R. Vera-Graziano, A. Martinez-Richa, Characterization of bone cements prepared with functionalized methacrylates and hydroxyapatite, J. Biomater. Sci. Polymer. Edn 12 (8) (2001) 893−910.
[79] A. Canul-Chuil, R. Vargas-Coronado, J.V. Cauich-Rodríguez, A. Martínez-Richa, E. Fernandez, S.N. Nazhat, Comparative study of bone cements prepared with either HA or α-TCP and functionalized methacrylates, J. Biomed. Mater. Res. 64B (2003) 27−37.
[80] L. Morejón, A.E. Mendizábal, J.A.D. García-Menocal, M.P. Ginebra, C. Aparicio, F.J.G. Mur, et al., Static mechanical properties of hydroxyapatite (HA) powder-filled acrylic bone cements: effect of type of HA powder, J. Biomed. Mater. Res. 72B (2) (2004) 345−352.
[81] M. Saito, A. Maruoka, T. Mori, N. Sugano, K. Hino, Experimental studies on a new bioactive bone cement: hydroxyapatite composite resin, Biomaterials 15 (2) (1994) 156−160.
[82] R. Labella, M. Braden, S. Deb, Novel hydroxyapatite-based dental composites, Biomaterials 15 (15) (1994) 1197−1200.
[83] M. Kobayashi, T. Nakamura, S. Shinzato, W.F. Mousa, K. Nishio, K. Ohsawa, et al., Effect of bioactive filler content on mechanical properties and osteoconductivity of bioactive bone cement, J. Biomed. Mater. Res. 46 (4) (1999) 447−457.
[84] C. Santos, Z.B. Luklinska, R.L. Clarke, K.W.M. Davy, Hydroxyapatite as a filler for dental composite materials: mechanical properties and in vitro bioactivity of composites, J. Mater. Sci. Mater. Med. 12 (2001) 565−573.
[85] Y. Shikinami, M. Okuno, Bioresorbable devices made of forged composites of hydroxyapatite (HA) particles and poly-l-lactide (PLLA): part I. Basic characteristics, Biomaterials 20 (9) (1999) 859−877.
[86] Z. Hong, P. Zhang, C. He, X. Qiu, A. Liu, L. Chen, et al., Nano-composite of poly(l-lactide) and surface grafted hydroxyapatite: mechanical properties and biocompatibility, Biomaterials 26 (2005) 6296−6304.
[87] N.H. Ladizesky, E.M. Pirhonen, D.B. Appleyard, I.M. Ward, W. Bonfield, Fibre reinforcement of ceramic/polymer composites for a major load-bearing bone substitute material, Compos. Sci. Technol. 58 (1998) 419−434.

[88] W.J. McGregor, K.E. Tanner, W. Bonfield, M. Bonner, L.S. Saunders, I.M. Ward, Fatigue properties of isotropic and hydrostatically extruded HAPEX™, J. Mater. Sci. Lett. 19 (2000) 1787−1788.

[89] M. Bonner, L.S. Saunders, I.M. Ward, G.W. Davies, M. Wang, K.E. Tanner, et al., Anisotropic mechanical properties of oriented HAPEX™, J. Mater. Sci. 37 (2002) 325−334.

[90] R.A. Sousa, R.L. Reis, A.M. Cunha, M.J. Bevis, Processing and properties of bone-analogue biodegradable and bioinert polymer composites, Compos. Sci. Technol. 63 (2003) 389−402.

[91] D.T. Reilly, A.H. Burstein, The elastic and ultimate properties of compact bone tissue, J. Biomechanics 8 (1975) 393−405.

[92] S.C. Cowin (Ed.), Bone Mechanics Handbook, CRC Press, Boca Raton, 2001.

[93] E.F. Morgan, T.M. Keaveny, Dependence of yield strain of human trabecular bone on anatomic site, J. Biomechanics 34 (2001) 569−577.

[94] T.M. Keaveny, E.F. Morgan, G.L. Niebur, O.C. Yeh, Biomechanics of trabecular bone, Annu. Rev. Biomed. Eng. 3 (2001) 307−333.

[95] R.J. Kane, G.L. Converse, R.K. Roeder, Effects of the reinforcement morphology on the fatigue properties of hydroxyapatite reinforced polymers, J. Mech. Behav. Biomed. Mater. 1 (3) (2008) 261−268.

[96] FDA public health notification: life-threatening complications associated with recombinant human bone morphogenetic protein in cervical spine fusion, July 1, 2008.